Experimental results on low-energy photon-atom scattering and a critical analysis of the data in the vicinity of K-absorption edges

S. K. Ghose, M. Ghose,* S. S. Nandi, A. C. Nandi, and N. Choudhuri
Department of Physics, North Bengal University, Darjeeling, West Bengal, 734 430 India
(Received 28 August 1989)

Results for the atomic elastic scattering of photons of 59.54 keV lying in the vicinity of K-absorption edges of rare earths ($_{68}$Er and $_{70}$Yb) are presented. An assessment of all existing experimental results published in the last few years has been made in terms of some of the most important calculations on photon–bound-electron collisions as a function of photon energy and momentum transfer that have been developed in the 1980s. The analysis presents the trend of behavior of the theoretical cross section as the incident photon energy crosses the K-shell photoionization thresholds of the scattering atomic system.

I. INTRODUCTION

The elastic scattering of photons in the x-ray and low-energy γ-ray regions by atomic bound electrons in the vicinity of atomic K edges has been investigated in recent years. In the energy region below 100 keV the scattering by bound electrons near the edges has been in a state of uncertainty due to problems arising from experimental techniques as well as theoretical methods. New calculations of dispersion corrections[1–4] to scattering cross sections near K edges made by a number of authors have encouraged new experimental studies on elastic photon scattering in the energy region below 100 keV. This paper includes new results for elastic photon scattering on a number of new elements with their K edges near the photon energy 59.54 keV and a critical analysis of similar experimental data published by other groups during the last few years.

II. THEORETICAL BACKGROUND

Photon-atom elastic scattering by atomic bound electrons, known as Rayleigh scattering, is expressed in the simpler atomic form factor approach by writing the differential cross section in the form

$$\frac{d\sigma^R}{d\Omega}=\frac{d\sigma^T}{d\Omega}|f(q)|^2$$

where $d\sigma^T/d\Omega=\frac{1}{2}r_0^2(1+\cos^2\theta)$, σ^R represents the photon-bound electron total scattering cross section, $r_0=e^2/mc^2$, the classical electron radius, θ is the scattering angle, $q=mcq'=2(\hbar\omega/c)\sin\theta/2$, $\hbar\omega$ is the incident photon energy, and q' is the change in photon momentum for the scattering process (i.e., momentum transferred to the atom by the scattering). The atomic form factor $f(q)$ for a spherically symmetric atom is given by

$$f(q)=4\pi\int_0^\infty\rho(r)\frac{\sin(qr)}{(qr)}r^2dr$$

where $\rho(r)$ is the charge number density satisfying the condition

$$4\pi\int_0^\infty\rho(r)r^2dr=1\ .$$

If the elastic scattering is due to a photon of energy very close to the atomic energy level, photon-resonant scattering will occur. The scattering power of the atom represented by $f(q)$ has to be modified by two correction terms, one arising from the proximity of the incident photon energy to the binding energy of the bound electron scattering the photon, and the second one representing absorption due to damping of the incident photon in the vicinity of the resonance level. With these two correction terms the true atomic scattering factor is written as

$$f_{\text{true}}=f(q)+f'+if''\ ,$$

where $f(q)$ is the atomic scattering factor far from any resonant bound electron energy level. f' is a real number representing the dispersion effect in scattering near the resonant level and if'' is an imaginary number representing the absorptive part of the dispersion effect in elastic scattering near a resonant state of the bound scattering electron.

III. WORK ON DISPERSION EFFECTS IN ELASTIC PHOTON SCATTERING

The initial work in the x-ray regime has been summarized by Compton and Allison in their book[5] which was extended to include the work of Honl.[6] In the extension of Honl's work, the real and imaginary parts of the dispersion correction (denoted by f' and f'') were predicted to depend on the photon frequency and momentum transfer as the following:

$$f_{\text{true}}(\omega,q)=f(\omega,q)+f'(\omega,q)+if''(\omega,q)\ .$$

However, the momentum transfer dependence had not been tested experimentally and more recent theoretical treatments do not support the predictions of Wagenfeld,[7] that f' and f'' are dependent on the momentum transfer. The determination of the dispersion corrections for the

case with $q \neq 0$ is based on the following relationships obtained in the dipole approximation:

$$f''=\frac{\omega}{4\pi r_0 c}\sigma_{Ph}(\omega), \quad f'=\frac{1}{2\pi^2 r_0 c}\mathrm{P}\int_{\omega_k}^{\infty}\frac{\omega'^2\sigma_{Ph}(\omega')}{\omega^2-\omega'^2}d\omega' ,$$

where $\sigma_{Ph}(\omega)$ is the photoelectric cross section, ω is the photon angular frequency, ω' is the angular frequency corresponding to the bound electron atomic level, c is the velocity of light, and P refers to the principal value of the integral.

The relativistic calculation of dispersion corrections f' and f'', based on the Dirac-Slater model calculation of photoelectric cross sections, were found by experiments to be inadequate. Cromer and Liberman,[1-3] however, have published improved calculations based on the Dirac-Hartree-Fock-Slater (DHFS) model.

The scattering matrix formalism of Brown and Meyers[8] and Kissel, Pratt, and Roy[9] using the DHFS model have provided extensive numerical calculations of whole-atom photon–bound-electron elastic scattering cross sections and also have given two schemes for applying dispersion corrections $f'(\omega,0)$ and $f''(\omega,0)$ at scattering angles with nonzero momentum transfer ($q \neq 0$). The method for applying $f'(\omega,0)$ and $f''(\omega,0)$ at higher scattering angles ($q \neq 0$) has not been tested. The present paper will test the predictions of Kissel and Pratt as well as very recent results of dispersion corrections[4] for an assessment in terms of recent experiments done over the last few years.

IV. PRESENT AND OTHER RECENT EXPERIMENTS

A sensitive intrinsic germanium detector (crystal specifications: 100-mm^2 active area, 7-mm thickness, 3.5-mm distance from detector to crystal window face) has been used for precision measurements of the photon-atom interaction replacing the previous NaI detector system because the resolution of the present detector system has been improved to 176 eV [full width at half maximum (FWHM)] for a photon energy of 5.89 keV. These improvements helped carry out measurements with an accuracy at the level of 5%. The experiments were carried out using a 10-mCi ^{241}Am source which emits γ rays with an energy of 59.54 keV. With this source a very accurate determination of the number of elastically scattered photons is possible, as these are well separated in the scattered spectrum from the component of inelastically scattered photons. The ^{241}Am source was placed in a lead shield housing of an adequate thickness permissible by the geometry at each angle in order to minimize the background reading. The housing has a conical bore with a length of 30 cm and a diameter of 2 cm as shown in Fig. 1. The angle of scattering (θ) and the angle (ψ) between the direction of incident beam and the scatterer were measured very carefully and accurately each time by telescopic arrangement. Each setting was checked to adjust the source, the scatterer, and the detector in the same horizontal plane. Background reading (without the scatterer at the scatterer holder) was always taken before and after each measurement. The average background

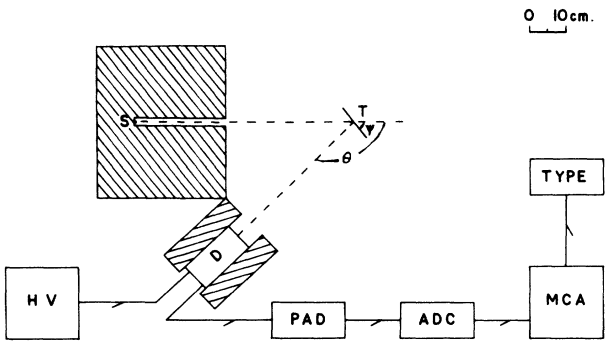

FIG. 1. Schematic diagram of the experimental arrangement S, source; T, target; D, detector; HV, high voltage; PAD, pulse amplitude discriminator; ADC, analog-to-digital converter; MCA, multichannel analyzer.

result was subtracted from the reading obtained with the scatterer at the position of the scatterer holder. The position of the particular channels in the multichannel analyzer (MCA) in which the coherent component peak appeared was tested before and after the experiment to check for any channel shift. The distance (r_1) between the source and the scatterer and the distance (r_2) between the scatterer and the detector were always kept equal. Simultaneously, the relation between θ and ψ was always $\psi=\theta/2$. These two adjustment were done to satisfy the condition

$$\frac{r_1}{r_2}=\frac{\sin\psi}{\sin(\theta-\psi)} .$$

The target foils used have the following dimensions.

Target atom	Area (cm^2)	Thickness (cm)
Mo	25	0.01
Cd	25	0.005
Sn	19.63	0.01
Er	25	0.01
Yb	25	0.01
Ta	19.63	0.001

Measurements were made using an ND 1100 multichannel analyzer system coupled to a Ge-detector head at a conversion gain of 1024 with 512 channels and a spectrum storage time in the range 4–100 ks. At a large scattering angle θ, the expression for the differential elastic scattering cross section can be shown to be

$$\frac{d\sigma}{d\Omega}=\frac{4\pi N_s \sin\theta r_1^2 r_2^2}{N_{\mathrm{at}} I_0 \epsilon A_d}G(\theta) \tag{1}$$

where N_{at} is the number of scattering atoms in the target, N_s is the number of scattered photons per second (scattered into the infinitesimal solid angle $d\Omega$), I_0 is the number of monoenergetic photons that the source emits per second, A_d is the area of the detector, and $G(\theta)$ is the geometrical correction factor (obtained from Kahane, Bar-Noy, and Moreh[10]). For relection geometry

$$G(\theta)=\frac{1-e^{-\mu t[1/\sin\psi-1/\sin(\theta-\psi)]}}{\mu t[1/\sin\psi-1/\sin(\theta-\psi)]}$$

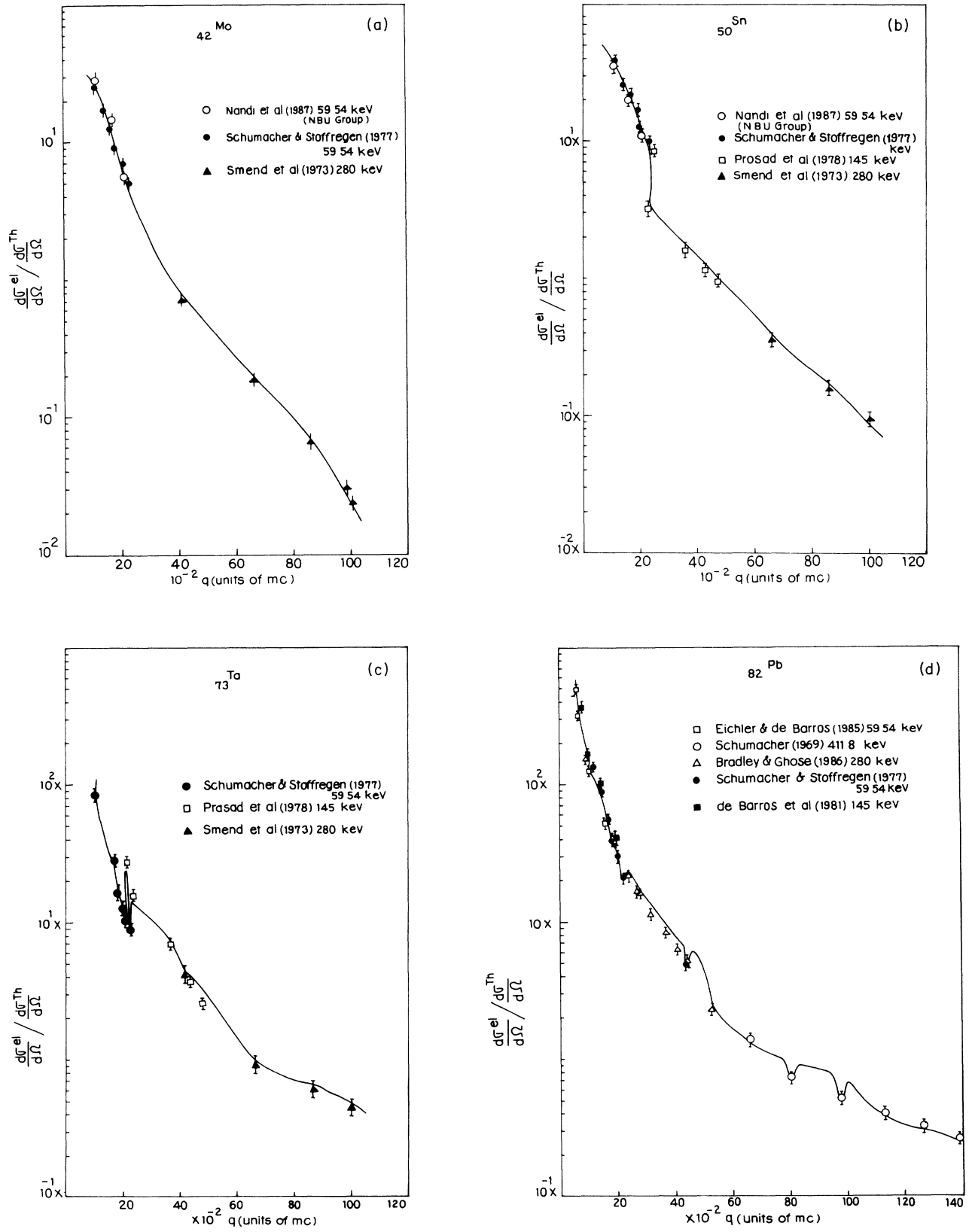

FIG. 2. Plot of $(d\sigma^{el}/d\Omega)/(d\sigma^{T}/d\Omega)$ against momentum transfer q in units of mc (a) for $Z=42$, (b) for $Z=50$, (c) for $Z=73$, and (d) for $Z=82$. The theoretical S-matrix predictions are plotted with the solid line and the experimental data points are shown by the symbols under the references as listed.

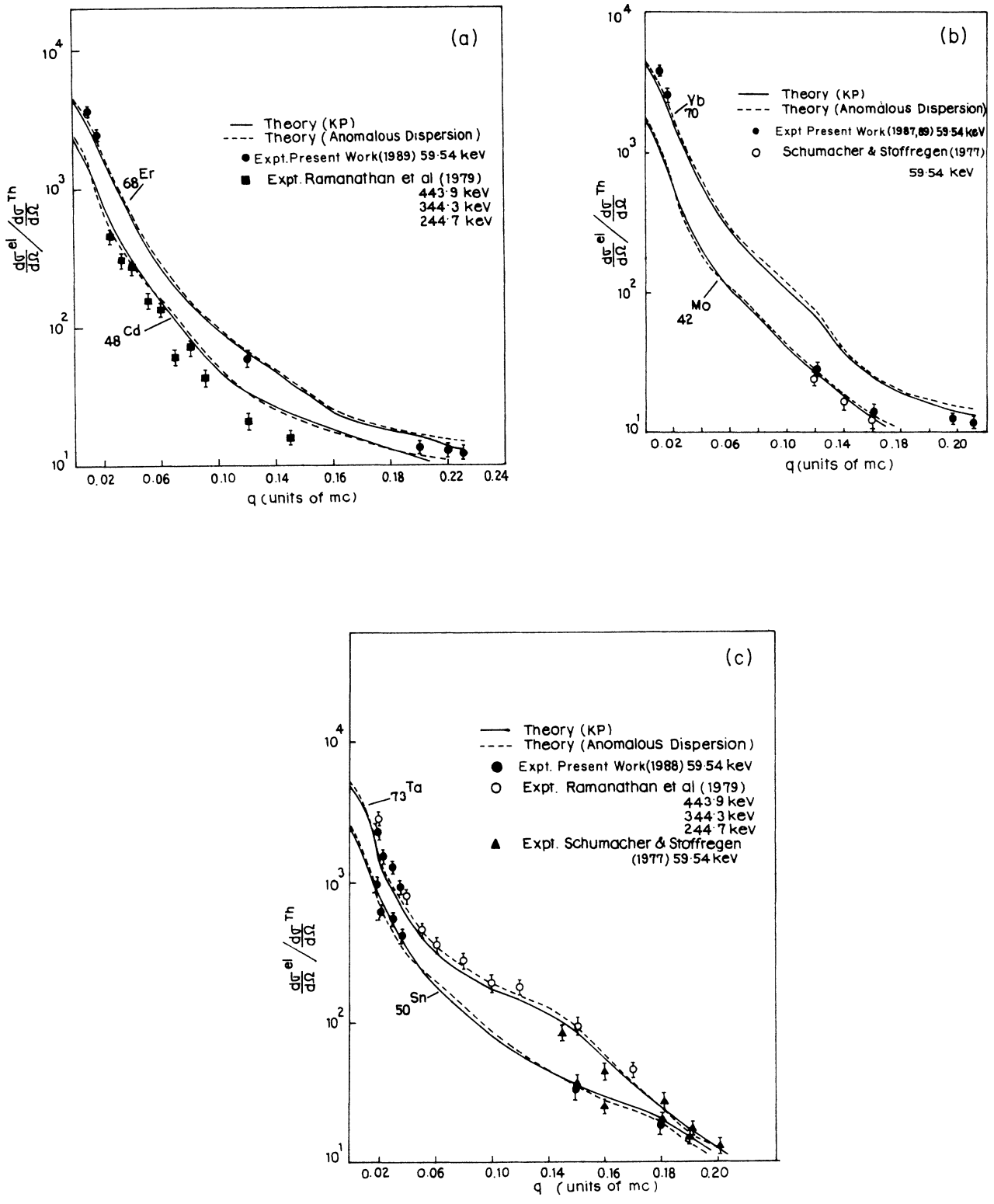

FIG. 3. Plot of $(d\sigma^{el}/d\Omega)/(d\sigma^{T}/d\Omega)$ aganst momentum transfer q in units of mc (a) for $Z=48$ and $Z=68$, (b) for $Z=42$ and $Z=70$, and (c) for $Z=50$ and $Z=73$. The theoretical S-matrix predictions are plotted with the solid line and the values obtained by using relativistic form factor corrected by anomalous dispersion terms of Creagh and McAuley are plotted with the dashed line. The experimental data points are shown by the symbols under the references as listed.

where μ (cm^{-1}) is the attenuation coefficient of the scatterer atom for incident photons and t (cm) is the thickness of the scatterer. An auxiliary experiment was carried out to determine the direct photon beam counts by keeping the intrinsic Ge detector at a large distance R. The direct photon beam count N_{Ge} is used in the formula connecting the source strength and the detector parameter expressed as

$$N_{Ge}=\frac{I_0}{4\pi R^2}A_d\epsilon\ . \tag{2}$$

When the result is compared with formula (1), the product $I_0\epsilon A_d$ is eliminated. In this way the determination of the efficiency (ϵ), source strength (I_0), and the detector area (A_d) was avoided.

Such high-resolution photon-atom scattering work in similar scattering geometry carried out during the last few years includes the work of Schumacher,[11] Smend, Schumacher, and Borchert,[12] Schumacher and Stoffregen,[13] Prasad *et al.*,[14] Ramanathan, Kennett, and Prestwich,[15] de Barros *et al.*,[16] Eichler and de Barros,[17] and Bradley and Ghose.[18] Bradley and Ghose, however,

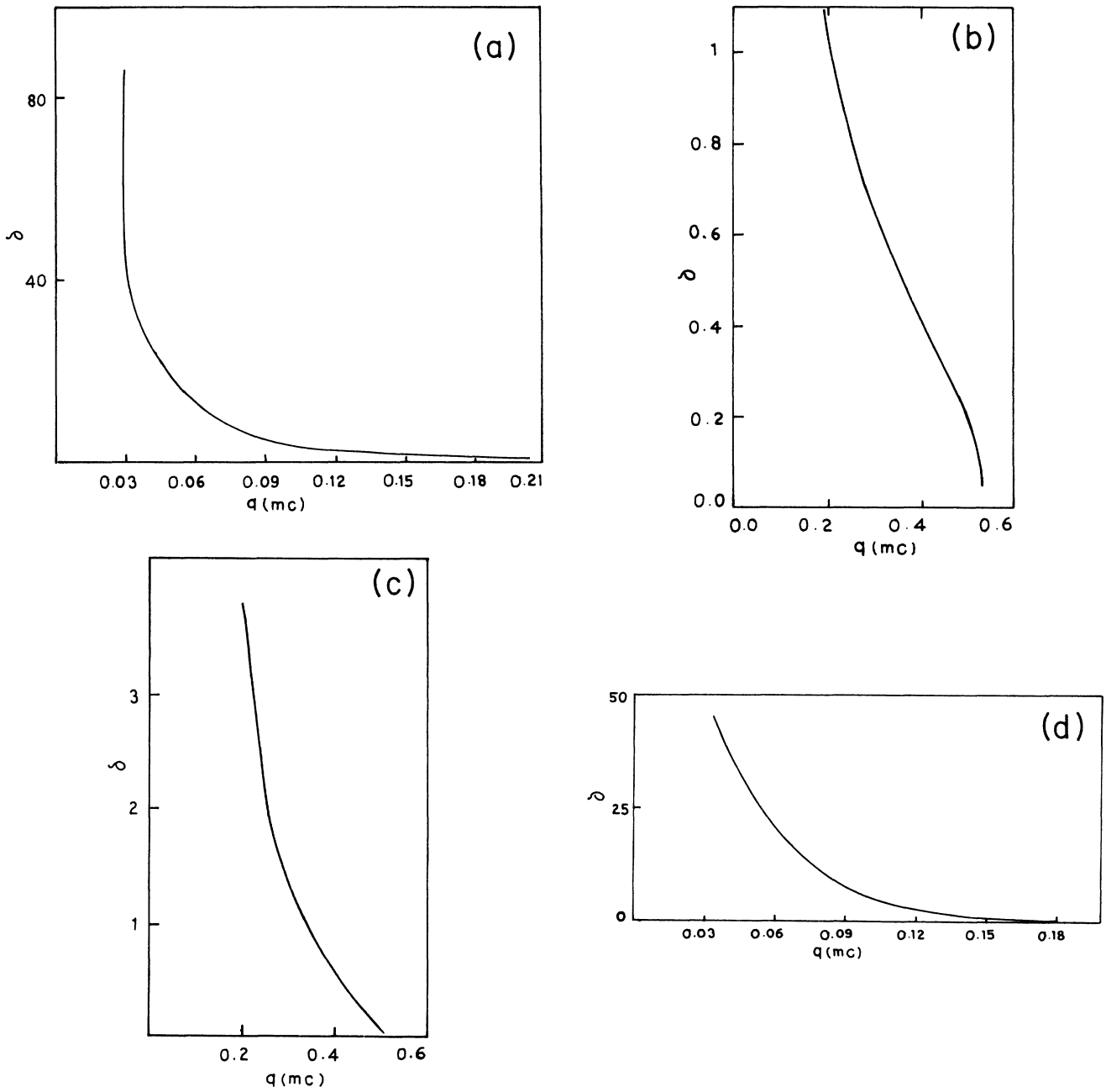

FIG. 4. Deviation δ of the experimental cross sections in units of $d\sigma^T/d\Omega$ from the corresponding theoretical values plotted against q in units of mc (a) for $Z=82$ with $E/E_k=0.675$, (b) for $Z=82$ with $E/E_k=3.17$, (c) for $Z=82$ with $E/E_k=4.679$, (d) for $Z=73$ with $E/E_k=0.883$, and (e) for $Z=50$ with $E/E_k=11.78$.

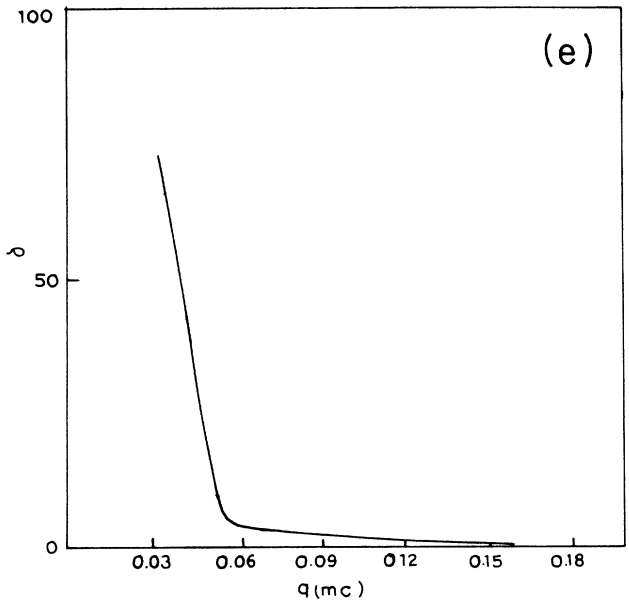

FIG. 4. (*Continued*).

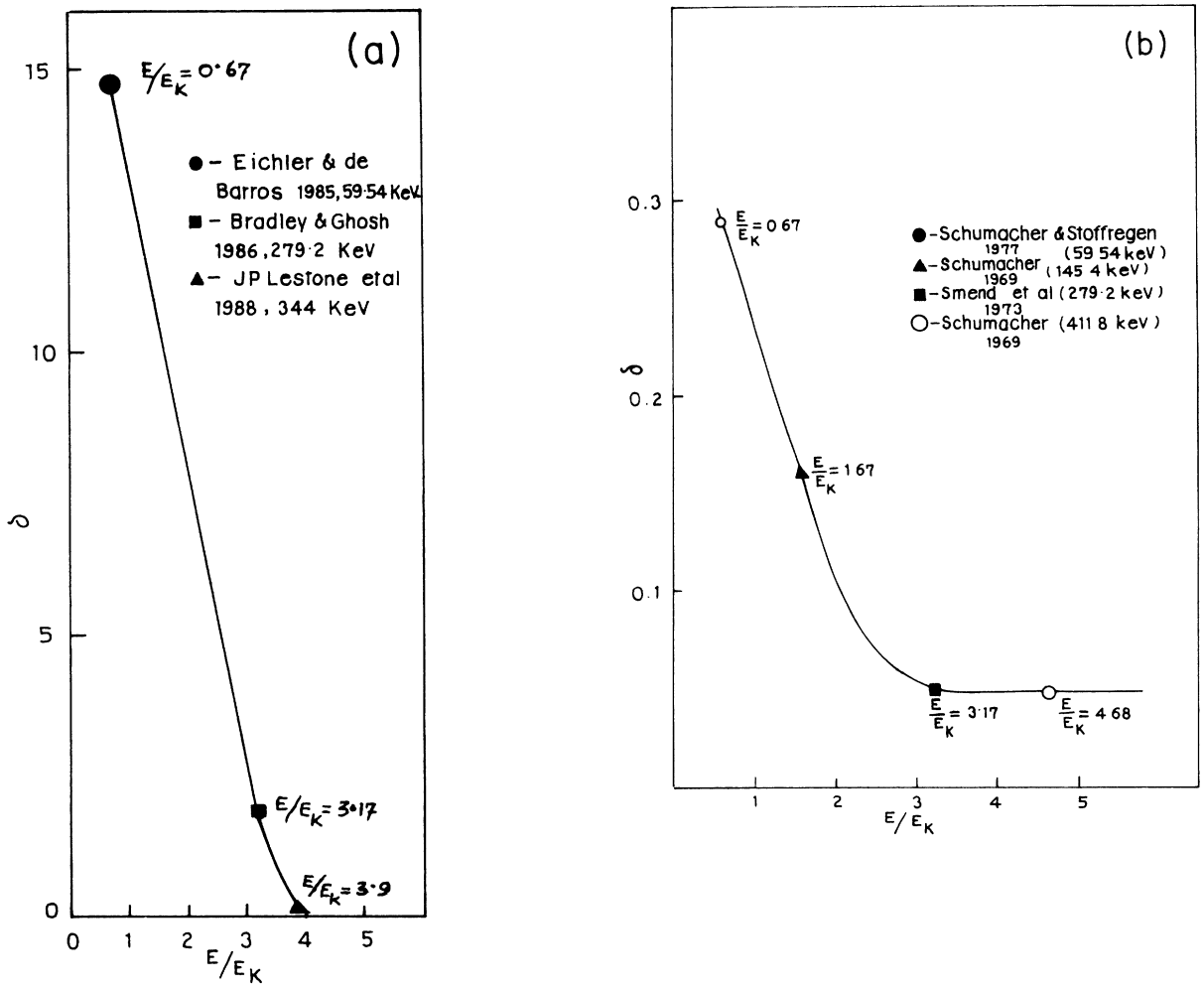

FIG. 5. Plot of δ against E/E_k for $Z=82$ (a) at the scattering angle $\theta=20°$ and (b) at the scattering angle $\theta=150°$.

have used scatterers in the shape of a surface of revolution about the source-detector axis. Lestone *et al.*[19] have performed elastic scattering measurements at angles between 2° and 45° using a polyenergetic γ-ray source containing ^{152}Eu and ^{154}Eu. At the small angles used in this investigation the elastic scattering peak and Compton peak overlap. The relative intensities of elastic and Compton scattering of a photon at an angle were therefore extracted using a least-squares method based upon experimentally measured Compton and elastic line shapes. Absolute elastic scattering cross sections were obtained using theoretical Compton cross sections for carbon (by normalizing to the theoretical carbon Compton cross section at 7°).

V. RESULTS AND DISCUSSION

For the analysis intended in this paper, we have presented the cross-section results from the set of complete measurements performed at a photon energy of 59.54 keV and have also included the experimental data of several other groups who have used high-resolution detection systems for other energies and scatterers: Schumacher[11] for 411.8 keV, Smend, Schumacher, and Borchert[12] for 280 keV, Ramanathan, Kennett, and Prestwich[15] for 244.7, 344.3, and 443.9 keV, de Barros *et al.*[16] for 145 keV, Eichler and de Barros[17] for 59.5 keV, Bradley and Ghose[18] for 280 keV, and J. P. Lestone *et al.*[19] for 344 keV. The cross-section data obtained from these experiments are compared with those predicted by theory in Figs. 2 and 3. The error bars on the data points include both systematic and statistical errors. In these graphs, the cross-section values have been expressed in units of Thomson cross section per electron and plotted as a function of the momentum transfer q in units of mc. The examination of the cross section as a function of momentum transfer allowed the experimental data of other groups on common targets to be considered even though the photon energies employed and the range of scattering angles investigated were different.

Some of the theoretical calculations (Kissel and coworkers,[9,20] Cromer and Liberman,[1-3] Wagenfeld,[7] and the most recent calculations of dispersion corrections by

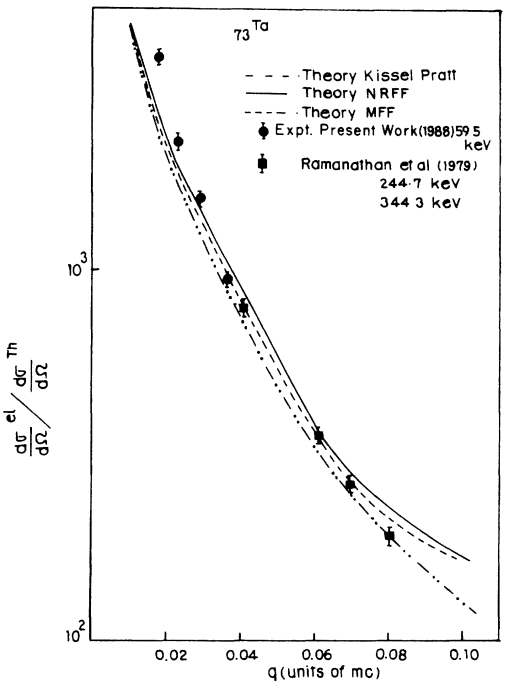

FIG. 6. Plot of $(d\sigma^{el}/d\Omega)/(d\sigma^{T}/d\Omega)$ against momentum transfer q in units of mc for $Z=73$. Theoretical predictions: nonrelativistic form factor (solid line), modified form factor (dashed line), and numerical Kissel-Pratt (dash-dotted line). Experimental points: 59.5 keV, Present Work (1988); 244.7 keV and 344.3 keV, Ramanathan, Kennett, and Prestwich (Ref. 15).

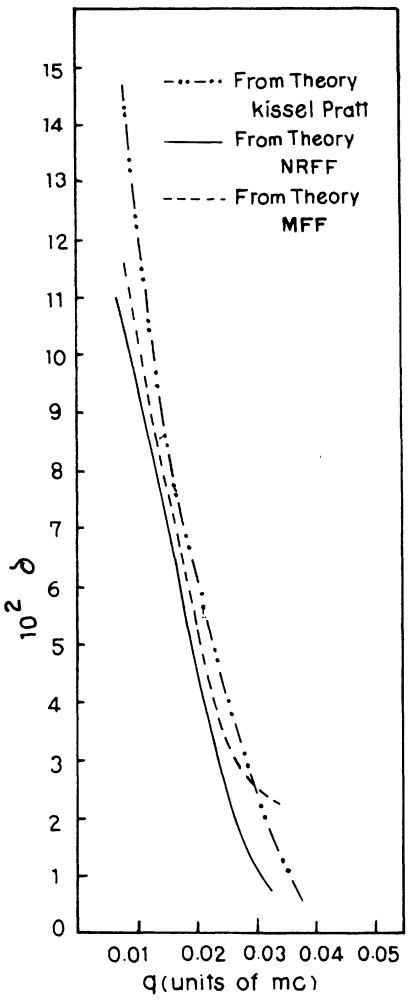

FIG. 7. Deviation δ of experimental $(d\sigma^{el}/d\Omega)/(d\sigma^{T}/d\Omega)$ from the corresponding theoretical values plotted against q in units of mc. The solid line denotes from nonrelativistic form factor, the dashed line denotes from modified form factor, and the dash-dotted line denotes from numerical Kissel-Pratt theory.

Creagh and McAuley[4]) include the corrections for the dispersion effect in photon-bound electron scattering. In Figs. 2 and 3 we have used only two theoretical models for comparison: the numerical S-matrix calculations of Kane *et al.*[21] and the relativistic form-factor calculations corrected for forward angle dispersion terms obtained from the calculations of Creagh and McAuley.[4] The computations of Kane *et al.* (referred to as the S-matrix formalism) are based on the exact numerical partial-wave method with the independent electron model. The simpler form-factor computation utilizes the atomic form factors obtained from the tabulations of Hubbell and Overbo[22] and the real and imaginary parts of dispersion corrections (f' and f'') as derived by Creagh and McAuley[4] based on attenuation measurements.

The dependence of the deviation δ of the experimental cross section from the corresponding theoretical value (both expressed in units of the Thomson cross section per electron) on the momentum transfer q (in mc units) is shown in Fig. 4 for each of the several E/E_k (the ratio of the incident photon energy to the target K-edge energy) values. In Figs. 5(a) and 5(b), on the other hand, values have been plotted against E/E_k for the scattering angles 20° and 150°, respectively. In the δ versus q graphs, however, we have not included all the cross-section results of measurements mentioned earlier. With a view to examining the data points with reference to the respective E/E_k values in the different regions of the q distribution we have chosen the experimental data from the results of measurements by various groups corresponding to a few representative q values from different regions. No attempt has been made to eliminate anomalous data sets.

We have further examined the simpler form-factor theories for the description of the elastic (Rayleigh) scattering of photons by the low-, medium-, and high-Z atoms by using (i) the calculations of Hubbell *et al.*[13] based on nonrelativistic Hartree-Fock wave functions and (ii) the calculations of Schaupp *et al.*[24] based on relativistic Dirac-Hartree-Fock-Slater wave functions. We find that for low- and medium-Z atoms and in the high-q range the distribution of $d\sigma/d\Omega$ is in good agreement with the nonrelativistic and modified form-factor results which are nearly the same as the results of numerical Kissel-Pratt calculations. But for scattering by high-Z atoms in the high-q region, the experimental results agree with the Kissel-Pratt predictions and differ considerably from both nonrelativistic and modified form-factor theories. The situation with respect to the two form-factor theories and the Kissel-Pratt predictions in the low-q range for $Z=73$ is displayed in Figs. 6 and 7.

An examination of the graphs reveals the following general trends.

(i) For incident photon energies above the K edges of target atoms ($E/E_k > 1$), theoretical predictions in different formalism appear to be in close agreement. The experimental results included in this analysis are generally in accord with theory.

(ii) At photon energies with E/E_k greater than 1 and in the momentum transfer range beyond $q=0.1$ the data points show better agreement with the various predictions of theory.

(iii) The experimental data exhibit larger deviations from theory for E/E_k less than 1 and at momentum transfer q below 0.1.

(iv) The points with E/E_k greater than 1 and at backward scattering angles agree reasonably well with theory. Significant deviations from theory seem to occur at forward scattering angles, particularly for E/E_k less than 1.

(v) At photon energies very nearly equal to the K-edge energy (i.e., $E/E_k \simeq 1$) experimental data are lacking. Elastic scattering measurements on ${}_{68}$Er ($E_k=57.49$ keV) using 59.54-keV photons at angles of 60°–150° showed that the cross-section results were 5–15 % lower than the S-matrix predictions over the whole range of scattering angles. Kane *et al.*[25] have reported measurements on ${}_{82}$Pb ($E_k=88.001$ keV) with 88.03-keV photons at the angle 125°. They obtained a cross-section value which is about 40% larger than the value predicted by S-matrix calculations.

We plan to examine the behavior of photon differential cross section on the vicinity of threshold energy positions in medium- and high-Z elements in future work.

ACKNOWLEDGMENTS

Support to S. K. Ghose by the University Grants Commission, India, is gratefully acknowledged.

*On leave from B. K. Girls' College, Howrah, West Bengal, India.

[1]D. T. Cromer and D. Liberman, J. Chem. Phys. **53**, 1891 (1970).

[2]D. T. Cromer and D. Liberman, Acta Crystallogr. Sect. A **37**, 267 (1981).

[3]D. T. Cromer and D. Liberman, J. Appl. Crystallogr. **16**, 437 (1983).

[4]D. C. Creagh and W. J. McAuley, *International Tables for Crystallography* (Kynoch, Birmingham, in press), Vol. C 4.2.6.

[5]X. Compton and X. Allison, *X-rays in Theory and Experiment* (Van Nostrand, New York, 1935).

[6]H. Honl, Ann. Phys. (Leipzig) **18**, 42 (1933).

[7]H. Wagenfeld, *Anomalous Scatttering*, edited by S. Ramaseshan and S. C. Abrahams (Mankasgaard, Copenhagen, 1975), pp. 12–23.

[8]G. E. Brown and D. F. Meyers, Proc. R. Soc. London, Ser. A **234**, 387 (1955).

[9]L. Kissel, R. H. Pratt, and S. C. Roy, Phys. Rev. A **22**, 1970 (1980).

[10]S. Kahane, T. Bar-Noy, and R. Moreh, Nucl. Phys. A **280**, 180 (1977).

[11]M. Schumacher, Phys. Rev. **182**, 7 (1969).

[12]F. Smend, M. Schumacher, and I. Borchert, Nucl. Phys. A **213**, 309 (1973).

[13]M. Schumacher and A. Stoffregen, Z. Phys. A **283**, 15 (1977).

[14]M. S. Prasad, G. K. Raju, K. N. Murty, V. A. N. Murty, and V. Lakshminarayana, J. Phys. B **11**, 3969 (1978).

[15]N. Ramanathan, T. J. Kennett, and W. V. Prestwich, Can. J. Phys. **57**, 343 (1979).
[16]S. de Barros, J. Eichler, M. Gaspar, and O. Goncalves, Phys. Rev. C **24**, 1765 (1981).
[17]J. Eichler and S. de Barros, Phys. Rev. A **32**, 789 (1985).
[18]D. Bradley and A. M. Ghose, Phys. Rev. A **33**, 191 (1986).
[19]J. P. Lestone, R. B. Taylor, P. Teamsomprasang, and I. Whittingham, Phys. Rev. A **37**, 3218 (1988).
[20]L. Kissel and R. H. Pratt, Lawrence Livermore Laboratory Report No. XRM-78-107 (1978), unpublished.
[21]P. P. Kane, L. Kissel, R. H. Pratt, and S. C. Roy, Phys. Rep. **140**, 75 (1986).
[22]J. H. Hubbell and I. Overbo, J. Phys. Chem. Ref. Data **8**, 69 (1979).
[23]J. H. Hubbell, W. J. Veigele, E. Briggs, R. T. Brown, and D. T. Cromer, J. Phys. Chem. Ref. Data **4**, 471 (1975).
[24]D. Schaupp, M. Schumacher, F. Smend, P. Rullhusen, and J. H. Hubbell, J. Phys. Chem. Ref. Data **12**, 467 (1983).
[25]P. P. Kane, G. Basavaraju, Saharsha M. Lad, K. M. Varier, L. Kissel, and R. H. Pratt, Phys. Rev. A **36**, 5626 (1987).